Microelectronics Reliability 52 (2012) 352–355

Contents lists available at ScienceDirect

Microelectronics Reliability

journal homepage: www.elsevier.com/locate/microrel

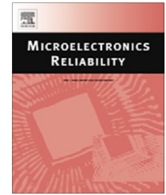

BCB-to-oxide bonding technology for 3D integration

S.L. Lin, W.C. Huang, C.T. Ko, K.N. Chen *

Department of Electronics Engineering, National Chiao Tung University, Hsinchu 300, Taiwan

ARTICLE INFO

Article history:
Received 27 April 2011
Received in revised form 11 May 2011
Accepted 13 May 2011
Available online 8 June 2011

ABSTRACT

Process optimization of BCB polymer to silicon oxide bonding was investigated. The suitable bonding temperature is about 300 °C, while bond failure of BCB-to-oxide bonding is observed starting from 400 °C. Bonding interface morphologies and bond strengths of BCB-to-oxide bonding were investigated as well. PECVD oxide to BCB bonding has better bonding quality than that of thermal oxide to BCB bonding. Si–O–Si bonds may be the reason of a strong BCB to oxide bonding. Water molecules link BCB and oxide surfaces during the initial contact, while Si–O–Si bonds are formed during bonding. This proposed mechanism of BCB-to-oxide bonding provides a guideline for polymer to oxide hybrid bonding technology in 3D integration.

© 2011 Elsevier Ltd. All rights reserved.

1. Introduction

Three-dimensional integrated circuit (3D IC) is a promising solution for decreasing the total global interconnect length that can limit IC performance. It refers to multiple conventional device layers/chips/wafers may be stacked vertically and electrically interconnected [1]. Based on current research and future outlook, 3D IC has the potential to dramatically enhance chip performance, functionality, and device packing density in integrated circuits (ICs) and micro electro mechanical systems (MEMS) applications [2].

Bonding technology is one of the key technologies in 3D IC. Bonding process in 3D integration can be performed for the structure enhancement by oxide or polymer bonding, or the electrical connection by metal bonding. In order to maximize the advantages of both bonding techniques, hybrid bonding, metal-to-metal bonding and oxide-to-oxide (or polymer-to-polymer) bonding, becomes a promising bonding technology in 3D IC [1,3]. It can provide a strong mechanical attachment and reduce the steps in the fabrication process. Among material usage for hybrid bonding, oxide-to-polymer bonding is a new concept in 3D IC without detailed studies.

In the choice of polymer material to bond with oxide, BCB seems a good candidate for hybrid bonding because of its excellent physical properties such as low dielectric constant, low moisture absorption, low cure temperature, high degree of planarization, low level of ionic contaminants, high optical clarity, good thermal stability, excellent chemical resistance, and good compatibility with various metallization systems [4,5]. The monomer structure of BCB is shown in Fig. 1 [6]. In this research, we investigated the process optimization and studied the bonding mechanism of BCB-to-oxide hybrid bonding for 3D IC applications.

* Corresponding author.
E-mail address: knchen@mail.nctu.edu.tw (K.N. Chen).

0026-2714/$ - see front matter © 2011 Elsevier Ltd. All rights reserved.
doi:10.1016/j.microrel.2011.05.008

2. Experimental

In this research, three groups of materials, 2 μm thermal oxide layer, 2 μm PECVD oxide layer, and 3 μm BCB polymer layer, were deposited and coated on Si wafers, respectively. All wafers with oxide and BCB layers were diced into 1.0 cm × 0.7 cm samples. Oxide and BCB samples were then stacked face-to-face by thermal-compression bonding. Based on oxide bonding mechanism [7], two flat, clean and smooth wafer surfaces are brought into contact and form bonds (Van der Waals bonds, covalent bonds, etc.). To form Van der Waals bonds or covalent bonds, the distance of two opposing surfaces must be less than 0.3–0.5 nm [7]. During the BCB-to-oxide bonding, the high bonding temperature would change BCB (thermal-setting epoxy) from solid phase to semi-liquid phase [8]. This deformation may bring two material surfaces in sufficient close contact and achieve bonding.

The surface contaminants may reduce the degree of the contact between two surfaces. Therefore, surface preparations are the key parameters for the bonding. To remove particles and impurities attached on the surface, all wafers received a 30 min DI water rinse plus spin dried. Then the oxide samples (the first and second groups) were dipped in DHF for 10 s to remove the native oxide followed by another 30 min DI water rinse and spin dried.

After surface preparation, PECVD oxide and thermal oxide samples were bonded directly to BCB samples (face-to-face), respectively, at 200 °C, 250 °C, 300 °C, 350 °C, and 400 °C for 30 min and 50 min. The bonding ambient was N_2 or atmosphere. All the bonding experiments were under a 50 N bonding force. After bonding, the bonding quality and bond strength between BCB and PECVD/thermal oxide were examined using razor test and pulling test, respectively. The two surfaces of bonded samples after razor/pulling test and bonded interfaces were analyzed by optical microscope and scanning electron microscope.

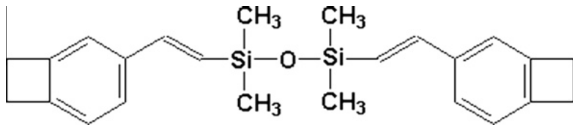

Fig. 1. BCB monomer chemical structure [6].

3. Morphology investigations

Fig. 2a–c shows images of BCB surfaces after thermo-compressional bonding process. The corresponding bonding conditions are (a) BCB to thermal oxide bonding at 200 °C for 30 min; (b) BCB to PECVD oxide bonding at 200 °C for 30 min; and (c) BCB to PECVD oxide bonding at 400 °C for 30 min. BCB surfaces were investigated by debonding the samples. In Fig. 2a, the BCB surface after bonding with thermal oxide at 200 °C/30 min has no prominent changes. It indicates that the BCB surface seems not interact with the thermal oxide surface at this bonding condition. The BCB surface after bonding with PECVD oxide at 200 °C/30 min, which failed the razor test, clustered into many of lumps, as shown in Fig. 2b. This phenomenon may represent that the BCB surface began to bond with the oxide surface. Comparing the surface morphologies in Fig. 2a and b, it is apparent that the change of PECVD to BCB bonding surface is more prominent than that of thermal to BCB bonding surface. Therefore, it is implied that "PECVD oxide to BCB bonding" is more easily bonded than "thermal oxide to BCB bonding" under the same bonding condition.

Fig. 2c shows the BCB surface after PECVD oxide to BCB bonding at 400 °C for 30 min. The BCB surface also shows the similar lumps in Fig. 2b. In addition, a peeling phenomenon is observed in the upper right corner of this image. This peeling area indicates that two surfaces in this area are already bonded and could not separate by the razor. In addition, the change in BCB surface color[1] (dark brown) shows the BCB chemical structure has been changed at 400 °C. Dark brown color and the less robust structure are the evidences that the bonding may fail under this bonding condition (400 °C/30 min).

Fig. 3 shows the cross-sectional SEM image of BCB to PECVD oxide bonding interface (bonding at 350 °C for 50 min). A well-bonded BCB-oxide sample without voids, and defects in the bonding interface area was achieved after this bonding condition. Therefore, by comparing the results in Figs. 2b, c, and 3, the bond quality does not always improve with the increase of bonding temperature.

4. Razor test analysis

To determine the optimum bonding temperature and duration, a series of bonding experiments with various bonding parameters were performed and investigated by the razor test and pulling test. The results of razor test in Table 1 shows that the quality of BCB-to-oxide bonding improves as the increase of bonding duration and temperature up to 350 °C. Below 350 °C, when the bonding temperature and time are increased, BCB does not flow yet, but already softens to achieve sufficiently close contact with the oxide surface to be bonded. After bonding, when temperature cools down, the BCB may transform back from semi-liquid phase into solid phase [7], but the BCB and oxide surfaces already form bonds and hold two samples together.

Table 1 also shows that PECVD oxide to BCB bonding is possible at 200 °C for 50 min bonding and at 250 °C for 30 min bonding.

[1] For interpretation of color in Figs. 2, 4–6, the reader is referred to the web version of this article.

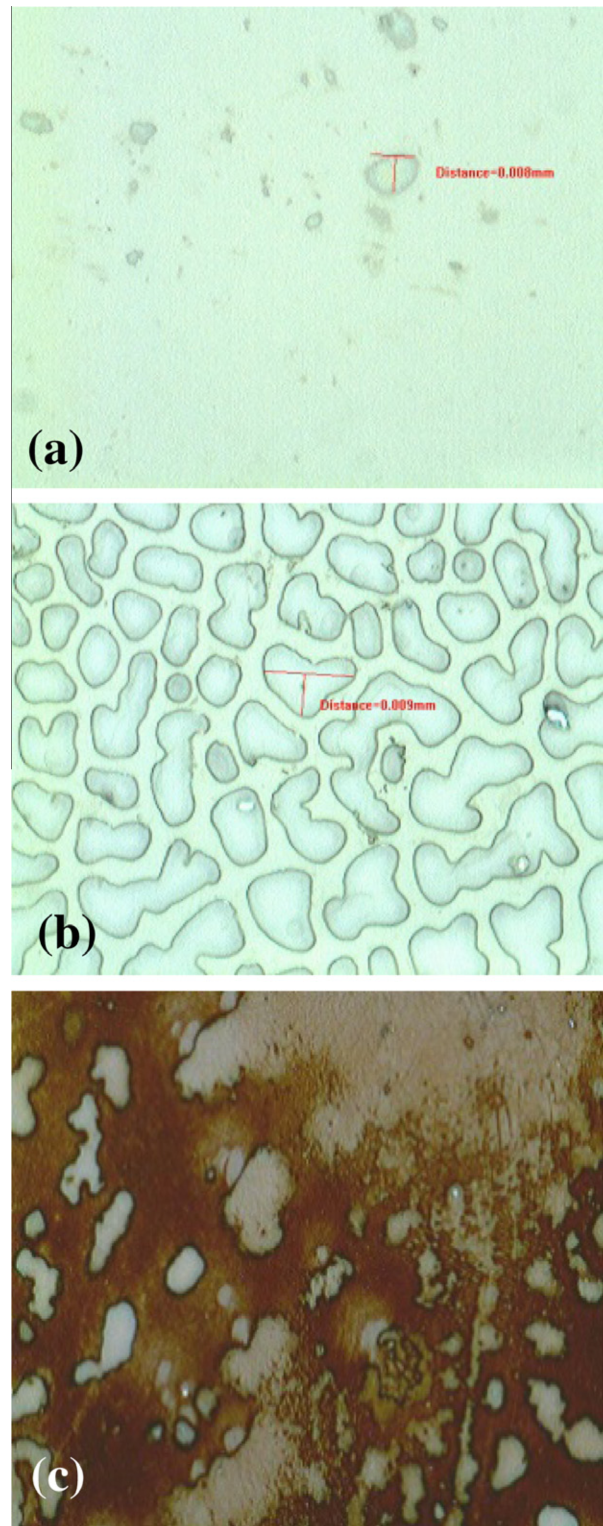

Fig. 2. OM images of BCB polymer surface after (a) BCB to thermal oxide bonding at 200 °C/30 min; (b) BCB to PECVD oxide bonding at 200 °C/30 min; (c) BCB to PECVD oxide bonding at 400 °C/30 min.

However, the thermal oxide to BCB bonding fails at these bonding conditions. It is suggested that "PECVD oxide to BCB bonding" is superior than "thermal oxide to BCB bonding" under the same bonding condition. The main reason for this phenomenon is that PECVD oxide film has more pores than thermal oxide one. These pores can provide sites for the gases, trapped after bonding

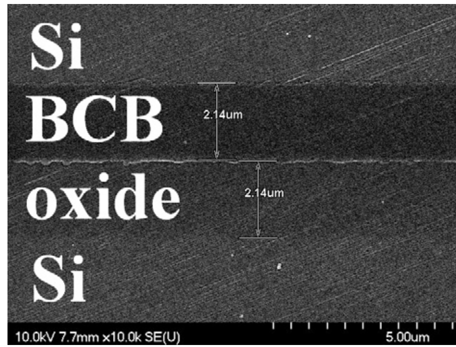

Fig. 3. SEM image of BCB to PECVD oxide bonding interface (350 °C/50 min).

Table 1
Panel A – Results of BCB to PECVD oxide bonding razor test. Panel B – Results of BCB to thermal oxide bonding razor test.

	200 °C	250 °C	300 °C	350 °C	400 °C
Panel A					
30 min	Fail	Pass	Pass	Pass	Fail
50 min	Pass	Pass	Pass	Pass	Fail
Panel B					
30 min	Fail	Fail	Pass	Pass	Fail
50 min	Fail	Pass	Pass	Pass	Fail

process, escape from the bonding interface. Therefore, the bonding strength is enhanced with the decrease of the number of bonding voids in the bonding interface [9].

In addition, porous oxide can help water molecules generated during bonding diffuse into the silicon. In general, silicon oxide layer is terminated by Si–OH on the surface. For silicon oxide to silicon oxide bonding at high temperature, the chemical reaction can be written as [9]:

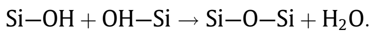

$$\mathrm{Si{-}OH + OH{-}Si \rightarrow Si{-}O{-}Si + H_2O.}$$

Since the pores provide sites for water molecules continue moving from bonding interface, the chemical reaction can further continue. It means that the Si–OH group can continue interacting and producing the new stronger Si–O–Si bonds [9]. This mechanism can be applied to BCB to oxide bonding. Therefore, these results in Table 1 not only suggest that the formation of Si–O–Si bonds is easier for porous PECVD oxide to BCB bonding than for thermal oxide to BCB bonding, but also give a hint that the Si–O–Si is the main bond to connect two surfaces.

5. Pulling test analysis

Samples of BCB to thermal oxide bonding with bonding conditions of 250 °C/50 min, 300 °C/50 min and 350 °C/50 min were investigated with the pulling test. Samples bonded with 250 °C/50 min and 300 °C/50 min conditions show bond strengths of 4.51 kgf and 40.08 kgf, respectively. However, although sample bonded at 350 °C for 50 min passes the razor test, its bonding strength is not strong enough to produce the pulling test data, as shown in Table 2. The strength of 300 °C bonding one is much larger than that of 250 °C bonding one. Therefore, it is suggested that the BCB polymer surface has a strong interaction with the silicon oxide surface during the temperature around 300 °C.

Table 2
Results of thermal oxide to BCB bonding pulling test.

	250 °C/50 min	300 °C/50 min	350 °C/50 min
Bonding strength	4.51 kgf	40.08 kgf	Fail

6. Mechanism of BCB to oxide bonding

To determine the bonding mechanism of BCB to oxide bonding, BCB samples were annealed between 250 °C and 475 °C with the spacing of 25 °C, and then analyzed by FTIR. Wavenumber region below 2000 cm^{-1}, the so-called fingerprint of the whole molecule, of BCB were investigated. Due to relatively large BCB molecule, the fingerprint region contains numerous partially overlapping peaks [10]. Because the FTIR spectrums of BCB between 250 °C and 325 °C remain the same, only FTIR analysis of BCB samples annealed between 325 °C and 475 °C are shown in Fig. 4.

As the temperature increased from 325 °C to 450 °C, the two dominant peaks located at wavenumbers of 805 cm^{-1} and 1263 cm^{-1}, which correspond to epoxy rings, decreased sharply [11]. As the temperature reached 400 °C, the epoxy ring in BCB almost dissociated [11]. This indicates that the cross-linking between two adjacent monomers in BCB had almost disappeared at 400 °C, which may affect the bonding quality at this temperature. In Table 1, it is evident that BCB-to-oxide bonding would fail when temperature reaches 400 °C.

Fig. 5 shows the Fourier transform infrared spectroscopy (FTIR) analysis of BCB samples as the temperature increased from 375 °C

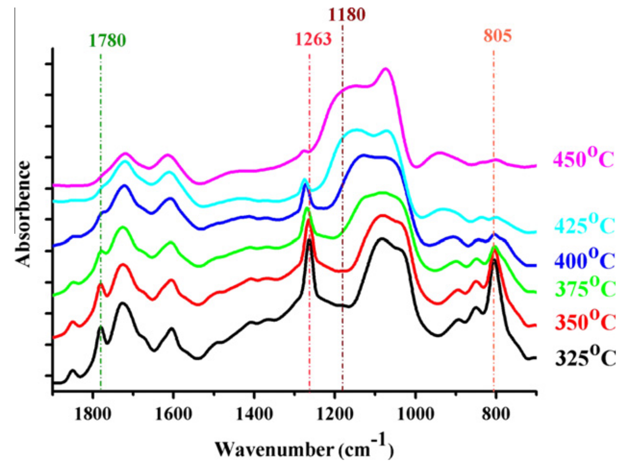

Fig. 4. FTIR diagram of BCB polymer surface structures annealed at 325 °C, 350 °C, 375 °C, 400 °C, 425 °C and 450 °C.

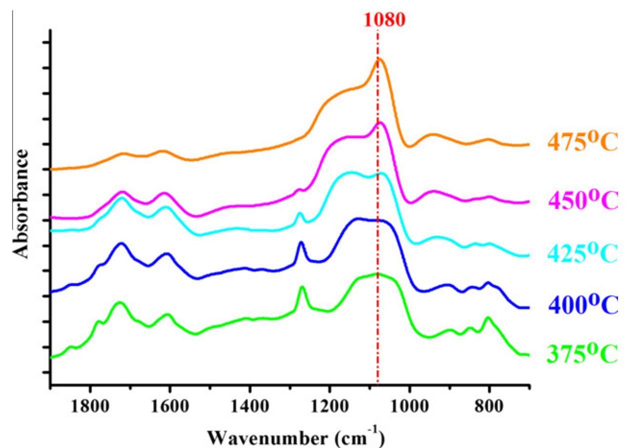

Fig. 5. FTIR diagram of BCB polymer surface structure annealed at 375 °C, 400 °C, 425 °C, 450 °C and 475 °C.

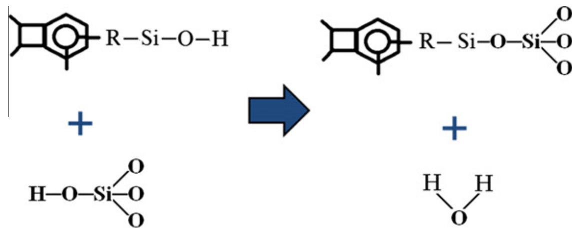

Fig. 6. The proposed reaction of BCB polymer surface to silicon oxide surface bonding.

to 475 °C. Contrast to the dissociation of epoxy rings in Fig. 4, it is clear that wavenumber 1080 cm^{-1}, representing Si–OR bonds [11], became dominant with the increase of temperature. Results from Figs. 4 and 5 suggest that the BCB structure in the temperature range would start to discompose but with the appearance of Si–OR bonds. Similar to the mechanism of silicon oxide bonding [12], when BCB surface and silicon surface contact together initially, the water molecules become bridges between the surfaces. During bonding, weak silanol bonds (Si–OH) are replaced with strong siloxane-covalent bonds (Si–O–Si) by the condensation reaction. The proposed reaction of BCB surface bonding to the oxide surface is shown in Fig. 6.

7. Conclusions

In summary, the suitable temperature range for BCB to oxide bonding is around 300 °C. The proposed mechanism of BCB to oxide bonding is due to the formation of Si–O–Si bonds of BCB. However, the decomposition of epoxy rings above the 400 °C results in the disappearance of the cross-linking between the BCB monomer and failures of bonding. In addition, PECVD oxide to BCB bonding is found to have better quality than that of thermal oxide to BCB bonding.

Acknowledgements

This research is supported by the National Science Council through Grant No. NSC 99-2628-E-009-093. The authors acknowledge sample preparation from H.C. Fu and facility supports from National Chiao Tung University and Industrial Technology Research Institute.

Reference

[1] Hua H, Mineo C, Schoenfliess K, et al. Exploring compromises among timing, power and temperature in three-dimensional integrated circuits. In: Proceedings of the 43rd annual design automation conference DAC; 2006.
[2] Niklaus F, Lu JQ, McMahon JJ, et al. Wafer-Level 3D integration technology platforms for ICs and MEMS. In: Proceedings of the 20th international VLSI; 2005.
[3] Jourdain A, Soussan P, Swinnen B, et al. Electrically yielding collective hybrid bonding for 3D stacking of ICs. In: Electronic components and technology conference; 2009.
[4] Chan KC, Teo M, Zhong ZW. Characterization of low-k benzocyclobutene dielectric thin film. In: Microelectronics international; 2003. p. 11–22.
[5] Scheck D, Rogers B, Garrou P, Dibbs M. Pre-develop bake for end point stabilization with photo-BCB polymers. In: International symposium on advanced packaging materials; 1998. p. 82–7.
[6] Garrou P, Scheck D, Im JH. Underfill adhesion to BCB (Cyclotene™) bumping and redistribution dielectrics. IEEE Trans Adv Pack 2000;23(3):568.
[7] Niklaus F, Stemme G, Lu JQ, Gutmann RJ. Adhesive wafer bonding. J Appl Phys 2006;99.
[8] Niklaus F, Kumar RJ, McMahon JJ, et al. Adhesive wafer bonding using partially cured benzocyclobutene for three-dimensional integration. J Electrochem Soc 2006;153(4):G291–5.
[9] Krauter G, Schumacher A, Gosele U. Low temperature silicon direct bonding for application in micromechanics: bonding energy for different combinations of oxide. Sens Actuators A 1998;70:271–5.
[10] Gunde MK, Hauptman N, Maček M, Kunaver M. The influence of hard-baking temperature applied for SU8 sensor layer on the sensitivity of capacitive chemical sensor. Appl Phys A 2009;95:673–80.
[11] Coates John. Interpretation of infrared spectra, a practical approach. In: Meyers RA, editor. Encyclopedia of analytical chemistry 2000:10815–37.
[12] Chen KN, Tan CS, Fan A, Reif R. Low-temperature direct CVD oxides to thermal oxide wafer bonding in silicon layer transfer. Electrochem Solid State Lett 2005;8(a):G1–4.